JOURNAL OF MOLECULAR RECOGNITION
J. Mol. Recognit. 2002; **15**: 6–18
DOI:10.1002/jmr.553

Functional characterization of an anti-estradiol antibody by site-directed mutagenesis and molecular modelling: modulation of binding properties and prominent role of the V_L domain in estradiol recognition

Stéphane Coulon[1], Jean-Luc Pellequer[2], Thierry Blachère[3], Martine Chartier[1], Elisabeth Mappus[3], Shu-wen W. Chen[2], Claude Yves Cuilleron[3] and Daniel Baty[1]*

[1]Institut de Biologie Structurale et de Microbiologie, 13402 Marseille Cedex 20, France
[2]Centre d'Energie Atomique Valrhô, Site de Marcoule, DSV/DIEP/SBTN, BP 17171, 30207 Bagnols-sur-Cèze, France
[3]INSERM U 329, Hôpital Debrousse, 29 rue Soeur Bouvier, 69322 Lyon Cedex 05, France

The high-affinity monoclonal anti-estradiol antibody 9D3 presents a specificity defect towards estradiol-3-sulphate and 3-glucuronide conjugates incompatible with use in direct immunoassays. The corresponding single-chain variable fragment (scFv), cloned and produced in *E. coli*, exhibited a 10-fold lower affinity for estradiol ($K_a = 1.2 \times 10^9$ M^{-1}) and a slightly increased specificity defect for the 3-position. Site-directed mutagenesis revealed critical residues involved in estradiol recognition and produced mutants exhibiting up to a 3-fold increase of the binding affinity for estradiol and up to a 2-fold decrease of the cross-reactivity with estradiol-3-sulphate. A comparative model of the antibody 9D3-estradiol complex was built in which the estradiol D-ring is buried into the binding pocket while the 3-, 6- and 7-positions are solvent exposed, agreeing with the lack of specificity for these three positions. Two potential alternative orientations of the A-ring, one close to CDR H3 and L2 loops, and the other one close to CDR H2 and L3 loops, have been considered for the docking of estradiol, none of which could be unambiguously privileged taking into account data from cross-reactivity measurements, photolabelling and mutagenesis studies. For both orientations, estradiol is stabilized by hydrogen bonding of the 17β-OH group with TyrL36, His89 and GlnH35 in the first case, or TyrL36, only, in the second case and by van der Waals contacts from TyrL91 with α- or β-face of estradiol, respectively, and from ValH95 and GlyH97 with the opposite face. To elucidate the molecular basis of antibody 9D3 specificity, as compared with that of another anti-estradiol antibody 15H11, single variable domains (V_H and V_L) and scFv hybrids have been constructed. The binding activity of V_L9D3 as well as the specificity of the V_L9D3/V_H15H11 hybrid, both similar to antibody 9D3, revealed a prominent role of V_L in estradiol recognition. These findings establish premises for antibody engineering to reduce cross-reactivity, especially with estradiol-3-conjugates. Copyright © 2002 John Wiley & Sons, Ltd.

Keywords: **antibody engineering; anti-steroid; estradiol; molecular modelling; photolabelling; site-directed mutagenesis**

Received 29 August 2001; revised 28 November 2001; accepted 29 November 2001

*Correspondence to: D. Baty, Institut de Biologie Structurale et de Microbiologie, Laboratoire d'Ingénierie des Systèmes Macromoléculaires, UPR 9027, CNRS, 31 chemin Joseph Aiguier, 13402 Marseille Cedex 20, France.
E-mail: baty@ibsm.cnrs-mrs.fr
Contract/grant sponsor: CNRS; *contract/grant number:* ACCSV5-9505207.

Abbreviations used: ANBA, (5-azido-2-nitrobenzoyl)amido; BSA, bovine serum albumin; CDR, complementary determining region; CMO, carboxymethyloxime; DHAS, dehydroepiandrosteronesulfate; DHT, 5α-dihydrotestosterone; DOC, 11-deoxycorticosterone; EA, ethylamido; FR, framework region; V_H, variable region of antibody heavy chain; V_L, variable region of antibody light chain; Fv, antibody variable fragment formed by non covalent association of V_H and V_L; CDR H1, H2, H3, heavy chain CDRs; CDR L1, L2, L3, light chain CDRs; IPTG, isopropyl-β-D-thiogalactopyranoside; mAb, monoclonal antibody; RIA, radioimmunoassay; scFv, single-chain variable fragment of an antibody formed by V_H and V_L covalently linked by a flexible peptide.

INTRODUCTION

Competitive radioimmunoassays using anti-estradiol antibodies and radiolabelled steroid tracers have become the most usual method to measure estradiol concentrations (Geisler *et al.*, 2000). However, monoclonal anti-estradiol antibodies with specificity and affinity adequate for use in direct immunoassays for clinical routine analysis have proved to be extremely difficult to obtain, compared with polyclonal antibodies. Steroids, owing to their low molecular mass (300–400 Da) are not immunogenic by themselves and have to be coupled covalently to a carrier macromolecule such as bovine serum albumin to be immunogenic. Therefore, antibodies recognising the coupled steroid may

have a stronger affinity against the immunogen than for the free steroid (Gani *et al.*, 1994). The access to high antibody specificity for a given steroid is particularly difficult since other steroids having very similar structures are also often present in serum, sometimes at much higher concentration. For example, estradiol differs from estrone only by the presence of a hydroxyl group at C17 position, instead of a ketone group while other usual metabolites such as 3-sulphate and 3-glucuronide differ only by conjugation on the C3 phenolic hydroxyl group. The presence of these steroid competitors requires that a direct immunoassay of estradiol in serum or urine samples should be realized with an anti-estradiol antibody very specific for both A- and D-ring extremities of estradiol. The specificity of an anti-steroid antibody depends on the position and structure of the linker introduced between the steroid and the carrier macromolecule (Yoon *et al.*, 1993) and is usually very poor for the region of covalent attachment on the haptenic steroid. Structural optimization of steroid hapten links introduced at intermediate positions has often been employed as a means to obtain polyclonal antibodies exhibiting an increased immunological recognition of the two characteristic C3 and C17 substituents, but failed to generate monoclonal antibodies specific for both A- and D-ring extremities. Moreover, some cross-reactions of the monoclonal anti-progesterone antibody DB3 have been explained by small but significant conformational changes in the paratope of the antibody that can accommodate different ligand orientations (Arevalo *et al.*, 1994).

Recent progress in molecular biology and phage-display technology (Marks *et al.*, 1992) have led to efficient methodologies of antibody engineering in order to modify antibody specificity and to improve binding affinity. The production of immunoglobulin fragments in heterologous expression systems is particularly suitable for the modification of the antigen-combining site. Various antibody constructions such as the antibody fragment (Fab), the antibody variable fragment (Fv) and the single-chain variable fragment (scFv) can be produced as functional and soluble proteins in *Escherichia coli* (Skerra and Plückthun, 1988; Plückthun, 1991). The production in *E. coli* of an anti-estradiol antibody is particularly attractive as a means to undertake structure–function studies of hapten–antibody interactions as a preliminary step toward reshaping of the combining site. Antigen-binding sites contain six hypervariable loops, forming the complementarity determining regions (CDRs) (Kabat *et al.*, 1991): CDR L1, L2 and L3 for the variable light chain domain (V_L) and CDR H1, H2 and H3 for the variable heavy chain domain (V_H). Except for CDR H3, CDRs have been classified into canonical structures (Chothia and Lesk, 1987; Chothia *et al.*, 1989). For both V_H and V_L, CDRs are loops protruding from a framework formed by four conserved regions: FR1, FR2, FR3 and FR4. The existence of known three-dimensional antibody structures like the one of the anti-progesterone antibody DB3 (Arevalo *et al.*, 1993) and of canonical structures of hypervariable loops, except for CDR H3, allows comparative models to be built with reasonable confidence for structure–function studies. These molecular models provide helpful data for the design of antibody engineering strategies, as shown for the 5A4 anti-cortisol antibody, for which Chames *et al.* (1998a) have constructed a phage-display library by parsimonious mutagenesis that led to an antibody with an improved specificity against cortisol.

In this study, a combination of site-directed mutagenesis, radioligand binding assays, photoaffinity labelling and molecular modelling was employed with the view of improving binding affinity and/or specificity of antibody 9D3 toward estradiol. A 3-fold increase in binding affinity and a 2-fold reduction in cross-reactivity with estradiol-3-sulphate could be obtained. The results also highlighted the unusual role played by the 9D3 light chain in binding affinity, thus establishing a new ground for future engineering of anti-estradiol antibodies of improved specificity.

EXPERIMENTAL PROCEDURES

Bacterial strain and phagemid

The bacterial strain *E. coli* HB2151 [Δ(*lac-pro*), *ara*, *nal*^{r}, *thi*/*F*′ *proAB*, *lacI*^{q}, *lacZ*Δ*M*15] was used as the bacterial host and was grown in 2YT culture medium (Miller, 1992). The phagemid vector pHENI (Hoogenboom *et al*., 1991) was used for the construction of pHENI-9D3, of pHENI-9D3 mutants and of PHENI-15H11.

Construction of the scFv

The 9D3 hybridoma was obtained from mice immunized with a 7-CMO-estradiol-BSA immunogen (Rolland de Ravel *et al.*, 2001). To construct the 9D3 scFv, V_H and V_L genes were amplified by PCR from κ light chain and γ heavy chain and inserted in the plasmid pBlueScript SK (Stratagene; Rousselot *et al.*, 1997). The 3′ primer used to amplify V_H contained the first part of the coding sequence for the flexible linker GSTSGSGKPGSGEGSTKG (Whitlow *et al.*, 1993). The 5′ primer used to amplify V_L contained the rest of the sequence (with 15 overlapping bases). The scFv was assembled by splice overlap extension PCR (Horton *et al.*, 1989). The primers used to amplify the 5′ and 3′ ends of the scFv gene introduced two restriction enzyme sites *Nco*I and *Eag*I, respectively. These sites were used to ligate the *scFv* gene into the pHENI phagemid vector to give pHENI-9D3 and pHENI-15H11.

Site-directed mutagenesis

Overlap PCR was used to build 9D3 mutants. Two PCRs were performed using pHENI-9D3 as the template and the primers 5′V_H9D3/3′ mutation-INF and 5′mutation-SUP/3′V_L9D3 (see below for primer sequences). The PCR products were purified with QIAquick (Gel Extraction kit from QIAGEN), mixed, and used as template in a final PCR using 5′V_H9D3/3′V_L9D3 primers. The final PCR product was inserted into the phagemid pHENI linearized with *Nco*I and *Eag*I. Clones were tested both by DNA minipreparation and restriction enzymes, for the presence of an insert of expected size and also for the production of a 30 kDa product using the anti-c-myc antibody as previously described (Hogenboom *et al.*, 1991).

Construction of hybrids and single domains

As described above, overlap PCR was used to build pHENI-V_H15H11/V_L9D3 and pHENI-V_H9D3/V_L15H11 with pHENI-9D3 and pHENI-15H11 as templates. *V_H9D3**, *V_L9D3*†, *V_H15H11*‡ and *V_L15H11*§ were amplified by PCR with the primer set 5′V_H9D3/3′V_H9D3, 5′V_L9D3/3′V_L9D3, 5′V_H15H11/3′V_H15H11, and 5′V_L15H11/3′V_L-15H11. The PCR products *V_H15H11-V_L9D3* and *V_H9D3-V_L15H11* were mixed to generate final hybrid gene products: *V_H15H11/V_L9D3* and *V_H9D3/V_L15H11*. In order to construct single domain antibodies, *V_H9D3*, *V_L9D3*, *V_H15H11* and *V_L15H11* were amplified by PCR with the primer set 5′V_H9D3/3′V_H9D3-*Eag*I, 5′*Nco*I-V_L9D3/3′V_L9D3, 5′V_H15H11/3′V_H15H11-*Eag*I, and 5′*Nco*I-V_L15H11/3′V_L-15H11. PCR products: *V_H15H11/V_L9D3*, *V_H9D3/V_L15H11*, *V_H9D3*, *V_L9D3*, *V_H15H11* and *V_L15H11* were inserted into the phagemid pHENI and clones were tested as described above.

Primer sequences

5′V_H15H11: CGGCCCAGCCGGCCATGGCCCAGGTTCTCCTACAAC; 5′V_H9D3: CGGCCCAGCCGGCCATGGCCGAGGTCCAGCTGCAGC; 3′V_H15H11: CCTGAACCAGGTTTACCAGAACCTGAGGTAGAACCTGAGGAGACTGTGAG; 3′V_H9D3: CCTGAACCAGGTTTACCAGAACCTGAGGTAGAACCTGCAGAGACAGTGAC; 5′V_L15H11: GGTAAACCTGGTTCAGGTGAAGGTAGTACTAAAGGTGACA TTGTGATGA; 5′V_L9D3: GGTAAACCTGGTTCAGGTGAAGGTAGTACTAAAGGTGACATCCAGATGAC; 3′V_L15H11-9D3: TTGTTCTGCGGCCGCCCG(TC)TTGAT(TC)TCCAG; 3′V_H9D3-*Eag*I: TTGTTCTGCGGCCGCTGCAGAGACAGTGACC; 5′*Nco*I-V_L9D3: GCCGGCCATGGCCGACATCCAGATGACTC; 3′V_H15H11-*Eag*I: TTGTTCTGCGGCCGCTGAGGAGACTGTGAGAG; 5′*Nco*I-V_L15H11: GCCGGCCATGGCCGACATTGTGATGACCC; 5′9D3H95-SUP: GTGGAAGG(GA)CAGACGGCTC; 3′9D3H95-INF: GGCCCGAGCCGTCTG(TC)CCTTCCAC; 5′9D3H97-SUP: AGAC(GT)CCTCGGGCCAC; 5′9D3H97-INF: GGCCCGAGG(CA)GTCTACCC; 5′9D3L91-SUP: CATCTT(TC)(GT)TTCTAGTATTC; 3′9D3L91-INF: ACTAGAA(AC)(GA)AAGATGACAG; 5′9D3L92-SUP: CATCTTTAT(AG)(CA)TAGTATTCC; 3′9D3L92-INF: ACTA(TG)(CT)ATAAAGATGACAG; 5′9D3L94-SUP: ATTCTAGT(TA)TGCCGTGGTCG; 3′9D3L94-INF: CCACCGAACGACCACGGCA(TA)ACTAGAATAAAG; 5′9D3L96-SUP: AGTATTCCG(TC)(GT)TTCGTTCGGTG; 3′9D3L96-INF: CCACCGAACGAA(CA)(AG)CGGAATACTAG; 5′9D3H96-SUP: GTGG AAGGGTA(GC)AAGGCTCGGGCC; 3′9D3H96-INF: GGCCCGAGCCTT(CG)TACCCTTCCAC; 5′9D3H97/H95-SUP: CTGTGGAAGG(GC)TAGACG(TG)CTCGGGCCAC; 3′9D3H97/H95-INF: GGCCCGAG(CA)CGTCTA(CG)CCTTCCACAG; 5′9D3-H33-SUP: TCACTAGATTT(TA)TGTCGCAATGGG; 3′9D3-H33-INF: TGCGACA(TA)AAATCTAGTGAA; 5′9D3-H35-SUP: TTATTTCG(AG)A(TA)TGGGTGAAGC; 3′9D3-H35-INF: TCACCCA(TA)T(TC)CGAAATAAATC; 5′9D3-H50-SUP: GGATTGGA(TC)(GT)TTTGGATCCT; 3′9D3-H50-INF: CCAAA(AC)(GA)TCCAATCCAC; 5′9D3-L50-SUP: CCTGGTCTAT(GC)A(TG)GCAAACACC; 3′9D3-L50-INF: AAGGTGTTTGC(AC)T(GC)ATAGACCAGG; 5′9D3-L53-SUP: AATGCAAACNGCTTAGCGGGAG; 3′9D3-L53-INF: CCCGCTAAGCNGTTTGCATT ATAG; 5′9D3-L89-SUP: TATTACTGTT(AT)TCTTTATTCTAG; 5′9D3-L89-INF: AGA ATAAAGA(TA)AACAGTAATAATTC.

RIA analysis

Cross-reactivities and antibody affinities were determined by RIA using a tritiated estradiol tracer. A culture of 100 ml of HB2151 cells harbouring phagemid was induced with IPTG 100 μM, at 30 °C, to an OD_{600} of 1 in 2YT medium containing 100 μg/ml ampicillin during 90 min. Cells were centrifuged, resuspended in 3 ml of phosphogel buffer (phosphate buffer 0.1 M pH 7.4; dextran 0.5 g/l; charcoal 5 g/l) and disrupted in a cell disruption equipment (Constant System Ltd, Warwick, UK) under 1000 bar pressure. The recovered sample was centrifuged (12 000g, 20 min, 4°C). Supernatant containing scFv was used for radioimmunoassays. In a 96-well plate (Nunc-Immuno-plate Maxisorp), coated with phosphogel buffer overnight at 4 °C, 100 μl of scFv dilution (1 up to 64) were mixed with 0.48 pmol (in 50 μl of phosphogel buffer) of [2,4,6,7-^{3}H]-estradiol (3.1 TBq/mmol; New England Nuclear, Boston, MA, USA) in 200 μl (final) of phosphogel buffer. The plate was incubated on rotator at least for 2 h at room temperature, then 10 min at 4 °C before addition of 100 μl of a suspension of dextran-coated charcoal. The plate was shaken at 4 °C on a rotator for 15 min, and centrifuged (1500g, 10 min at 4 °C). The radioactivity of each well (200 μl) was determined by liquid scintillation counting (PCS liquid scintillation, Amersham Pharmacia Biotech). The dilution corresponding to 50% of the bound radioactivity was chosen to calibrate the scFv concentration for the following binding assays. One hundred microliters of the appropriate concentration of scFv solution were mixed with 50 μl of different amounts of estradiol and estradiol-3-sulphate (0.002 up to 250 pmol in phosphogel buffer) in 96-well plates with 50 μl of [2,4,6,7-^{3}H]-estradiol. Controls without scFv and free estradiol were carried out to determine the amount of the specific [2,4,6,7-^{3}H]-estradiol not precipitated by charcoal. The last control with 50 μl of [2,4,6,7-^{3}H]-estradiol in 250 μl of phosphogel was performed to determine the amount of [2,4,6,7-^{3}H]-estradiol. The equilibrium constant for binding was determined by Scatchard plot analysis from the bound and free estradiol concentrations. Concentrations allowing 50% inhibition (IC_{50}) of the bound tracer were determined from the inhibition curves. The percentage of cross-reaction was given by the equation: (IC_{50} estradiol/IC_{50} competitor) × 100. Each measurement was made in triplicate with different antibody extracts for each scFv.

Molecular modelling and docking of estradiol

The Fv 9D3 model was built with a partially automatic procedure using the template structure of anti-lysozyme

*GenBank accession number: AY038362.
†GenBank accession number: AY038361.
‡GenBank accession number: AF001867.
§GenBank accession number: AF001868.

antibody D44.1 (PDB code, 1MLB; Braden *et al.*, 1994), which has a high sequence similarity. Side-chains were built and optimized using in-house programs. Briefly, side-chains were automatically replaced in the most common rotamer found in the library of Tuffery *et al.* (1991). A self-consistent linear search in rotamer space was performed, followed by a dihedral angle minimisation procedure using the Nelder-Meads simplex algorithm (Chen S-WW and Pelleques JL, unpublished results). Because of the similarity of CDR L3 from 9D3 with that from the anti-vascular endothelial growth factor antibody (rhumAb anti-VEGF; PDB code, 1CZ8), one of the high-resolution antibody structures that contains TrpL96 and TyrL91 (Chen *et al.*, 1999), this latter CDR L3 was incorporated into 9D3 (residues L89–L97), one of the high-resolution antibody structures that contains TrpL96 and TyrL91, by superimposing backbone atoms (N, Cα, C) of conserved β-strands (Roberts *et al.*, 1994). Compared to D44.1, CDR H3 of 9D3 is one residue shorter. Using the program Turbo-Frodo (Roussel and Cambillau, 1989), TyrH99 was deleted and an extended conformation for CDR H3 was modelled. Because of their poor geometry, regions L75–L84, L30–L32 and L66–L69 were rebuilt using the anti-lysozyme antibody D1.3 (PDB code, 1VFA; Bhat *et al.*, 1990).

Energy minimizations were done using the X-PLOR program (Brünger, 1992) with the all-atom force field CHARMM22 (Brooks *et al.*, 1983). Non-bonded interactions were limited to a radius of 13 Å, with the truncated functions for electrostatic and van der Waals terms set to 'shifted' and 'switched', respectively, with a cut-on of 9.5 Å and a cut-off of 12 Å. Conjugate gradient minimisations were considered convergent when the gradient reached 1.0 kcal/mol/Å^2 for side-chain optimization with the electrostatic term turned off, or 3.0 kcal/mol/Å^2 for all atoms with the electrostatic term turned on and a dielectric constant of 1.0. No histidines were doubly protonated in the model. Several cycles of refinements were performed using Turbo-Frodo, Xfit (McRee, 1992), and X-PLOR. The geometry of the model was analysed by the PROCHECK program (Laskowski *et al.*, 1993).

Molecular docking of the estradiol was performed using computer graphics and refined using a combination of rigid-body minimizations and distance restraints (noe statement in X-PLOR). Two possible alternative orientations of the steroid were retained, one (model A) corresponding to that found in the Fab 57-2-estradiol complex crystal structure (PDB code, 1JGL; Lamminmäki and Kankare, 2001) and the other one (model B) similar to that proposed in an earlier molecular model of the same antibody 57-2-estradiol complex (Lamminmäki *et al.* 1997). In model A, rigid-body minimization cycles included constraints from atom O17 of estradiol with atom Oη of TyrL36, atom Nε2 of HisL89, and atom Oε1 of GlnH35 (average distance of 3 Å). In model B, rigid-body minimization cycles included side-chain optimizations and a distance restraint between the atoms C9 of estradiol and Nε1 of TrpH47 was defined with an average distance of 7.6 Å (+0.1 Å, −0.6 Å).

Photolabelling experiments

Photoaffinity labelling of mAb 9D3 (Rolland de Ravel *et al.*, 2001) was performed with five photoreagents: 3-ANBA-ethylamido-carboxymethyloxy-[17α-^{3}H]-estradiol, 3-ANBA-ethyloxy-[17α-^{3}H]-estradiol, 6α-ANBA-[17α-^{3}H]-estradiol, 6β-ANBA-[17α-^{3}H]-estradiol and 7-ANBA-ethylamido-carboxymethyloxy-[17α-^{3}H]-estradiol, according to protocols similar to those reported for the anti-estradiol antibody 15H11 (Rousselot *et al.*, 1997). Photoaffinity labelled tryptic peptides isolated by immunopurification and HPLC were analysed by Edman sequencing and mass spectrometry.

RESULTS

Cloning of a scFv fragment of mAb 9D3

Gene regions coding for V_L and V_H domains were assembled by splice overlap extension PCR in a monocistronic form called scFv and inserted into the pHENI phagemid to give pHENI-9D3. The nucleotidic sequences were compared with the mouse immunoglobulin set from the ImMunoGeneTics database (reference directory: http://imgt.cines.fr:8104). The κ light chain belongs to Vκ12-41.01 family and the Jκ1.01 gene segment, and the γ heavy chain belongs to V_H1S12 family and the D-ST4 or IgHD-SP2 and J_H3.01 gene segments.

Sequence analysis of V_L and V_H domains of mAb 9D3

The amino acid sequences of the variable domains of H and L chains of anti-estradiol antibody 9D3 were aligned with those reported for two other anti-estradiol antibodies 15H11 (Rousselot *et al.*, 1997) and 57-2 (Lamminmäki *et al.*, 1997), the anti-cortisol antibody 5A4 (Le Calvez *et al.*, 1995) and the anti-progesterone antibody DB3 [Arevalo *et al.*, 1993; Fig. 1(a)]. The length of CDR H3 of the three anti-estradiol antibodies is very short, compared to other anti-steroid antibodies [Fig. 1(a)]. In particular, the 15H11 antibody exhibits the shortest CDR H3, which only contains three amino acids instead of six and seven residues for antibodies 9D3 and 57-2, respectively. Moreover, these three anti-estradiol antibodies are devoid of the usual salt bridge stabilizing the basis of the CDR H3 loop between ArgH94 and AspH101 residues as observed in most anti-hapten antibodies. Only anti-estradiol antibody 9D3 exhibits an ArgH94, whereas none of the three anti-estradiol antibodies contains acidic residues at position H101 (Asp or Glu). Antibodies 9D3 and 57-2 have a high level of identity for the V_L (90% for the entire V_L and 74% for the CDRs), whereas their V_H have only 51% sequence identity. These observations point to the hypothesis that differences in specificity of these two antibodies come from their V_H. The roles of the two variable domains of 9D3 are discussed below.

Specificity of mAb 9D3: cross-reactivity and photoaffinity labelling profiles

Cross-reactions of mAb 9D3 were measured with different estradiol derivatives and other steroids, using a tritiated estradiol tracer (Table 1). Steroids with modifications in D-ring, especially the 17-keto group of estrone and the 16α-hydroxyl group of estriol, are not recognized by antibody

Heavy chain V_H

```
        /          FR1           /    H1    /        FR2        /   H2   /                    FR3                   /       H3        /   FR4    /
        1       10        20        30          40        50             60        70   80            90        100              110
a       .        .         .        . ab        .         .  abc         .         .    . abc         .         .abcdefghijk       .
15H11   QVLLQQPITELARPGTSVKLSCKAS GYAFPS**H VMSWVKQISGQGLEWIGEI YP**RSGN SYYNENFKDRATLTADRSSNTVYMEVSSLTTEDSAVYFCGF G***************KE WGQGTTLTVSS
9D3     EVQLQQSGPELVKPGASVKMSCKAS GYTFTR**F ISQWVKQRPGQGLEWIGYL DP**YSGG PKYSEKFKGKATLTADIFSNTAYMELSSLTSEDSAVYFCGR VDGS************GH WGQGTLVTVSA
57-2    QIQLVQSGPELKKPGETVRISCKAS DYSFMT**S GMQWVQQMPGKGLKWIGWL NT**QSGV PEYAEDFKGRFAFSLETSATTAYLQINNLKNEDTATYFCAT WGGNS***********AY WGQGTTLTVSS
5A4     EVKLQESGTELVKPGASVKLSCKTS GFTFSS**R YMSWLKQKSGQSLEWIAWI YG**GTGG SNYNQKFTGKAQVTVDTSSSTVYMQFSSLTTEDSAIYYCAR HSVYGSSTPF*******DS WGQGTSVTVSS
DB3     QIQLVQSGPELKKPGETVKISCKAS GYAFTN**Y GVNWVKEAPGKELKWMGWI NI**YTGE PTYVDDFKGRFAFSLETSASTAYLEINNLKNEDTATYFCTR GDYVNWYF*********DV WGAGTTVTVSS

b
D44.1   QVQLQESGAEVMKPGASVKISCKAT GYTFST**Y WIEWVKQRPGHGLEWIGEI LP**GSGS TYYNEKFKGKATFTADTSSNTAYMQLSSLTSEDSAVYYCAR GDGNY***********GY WGQGTTLTVSS
1CZ8    EVQLVESGGGLVQPGGSLRLSCAAS GYDFTH**Y GMNWVRQAPGKGLEWVGWI NT**YTGE PTYAADFKRRFTFSLDTSKSTAYLQMNSLRAEDTAVYYCAK YPYYYGTSHWYF*****DV WGQGTLVTVSS
D1.3    QVQLQESGPGLVAPSQSLSITCTVS GFSLTG**Y GVNWVRQPPGKGLEWLGMI W***GDGN TDYNSALKSRLSISKDNSKSQVFLKMNSLHTDDTARYYCAR ERDYRL***********DY WGQGTTLTVSS
```

Light chain V_L

```
        /          FR1          /        L1        /       FR2       /  L2   /                 FR3                /     L3      /   FR4   /
        1       10        20        30              40         50         60        70      80         90             100
a       .        .         .        .abcdef          .          .          .         .       .          .   abcdef      .
15H11   DIVMTQSPASISVSLGDTVSITC HASQGIN******SNIG WLQLKPGKSFKGLMY HGNTLED GIPSRFSGSGSGGIYSLTINSLEFEDFAVYYC VQYAQFP******RT FGGGTRLEIKR
9D3     DIQMTQSPASLSASVGETVTITC RASGNIH******NYLA WYQQKQGKSPQLLVY NANTLAG GVPSRFSGSGSGTQFSLTINSLQPEDFGNYYC HLYSSIP******WS FGGGTRLEIKR
57-2    DIQMTQSPASLSASVGETVTITC RASGNIH******NYLA WYQQKQGKSPQLLVY NAKTLAD GVPSRFSGSGSGTQYSLKINSLQPEDFGTYYC HHFWSTP******WI FGGGTKLEVKR
5A4     DIVLTQSPAILSASPGEKVSMTC RATSSV*******SYMH WYQQKPGSSPKPWIY ATSNLAS GVPARFSGSGSGTSYSLTISRVEAEDAATYYC QQWSSNP******PT FGAGTKLELKR
DB3     DVVMTQIPLSLPVNLGDQASISC RSSQSLIHSNGN*TYLH WYLQKPGQSPKLLMY KVSNRFY GVPDRFSGSGSGTDFTLKISRVEAEDLGIYFC SQSSHVP******PT FGGGTKLEIKR

b
D44.1   DIELTQSPATLSVTPGDSVSLSC RASQSIS******NNLH WYQQKSHESPRLLIK YVSQSSS GIPSRFSGSGSGTDFTLSINSVETEDFGMYFC QQSNSWP******RT FGGGTKLEIKR
1CZ8    DIQLTQSPSSLSASVGDRVTITC SASQDIS******NYLN WYQQKPGKAPKVLIY FTSSLHS GVPSRFSGSGSGTDFTLTISSLQPEDFATYYC QQYSTVP******WT FGQGTKVEIKR
D1.3    DIVLTQSPASLSASVGETVTITC RASGNIH******NYLA WYQQKQGKSPQLLVY YTTTLAD GVPSRFSGSGSGTQYSLKINSLQPEDFGSYYC QHFWSTP******RT FGGGTKLEIKR
```

Figure 1. (a) Amino acid sequence alignment of V_H and V_L of 15H11 (anti-estradiol), 9D3 (anti-estradiol), 57-2 (anti-estradiol), 5A4 (anti-cortisol), and DB3 (anti-progesterone). (b) Amino acid sequence alignment of V_H and V_L of D44.1 (anti-lysozyme), 1CZ8 (rhumAb VEGF: anti-vascular endothelial growth factor), and D1.3 (anti-hen egg white lysozyme). The three-dimensional structures of these antibodies were used to construct the model of Fv 9D3. All residue numbering and loop definition (H1-H3; L1-L3) follows the scheme of Chothia and Lesk (1987).

Table 1. Specificity of monoclonal anti-estradiol antibody 9D3 for steroid analogues

Steroid and estradiol derivative	Cross-reaction (%)
Estradiol	100
Estradiol-3-sulphate	51
Estradiol-3-glucuronide	28
6-Oxoestradiol	36
6α-ANBA-estradiol	103
6β-ANBA-estradiol	33
7-Oxoestradiol	5
7-CMO-estradiol	11
Estrone	0.03
Estriol	0.3
Cortisol	<0.001
Testosterone	0.1
Progesterone	<0.001
DHT	0.2
DHAS	0.64
DOC	<0.001

The specificity was measured on the ascitic fluid. The percentage of cross-reactions was calculated as follows: (IC_{50} estradiol/IC_{50} analogue) × 100. The IC_{50} is the concentration of steroid necessary to obtain 50% of the control signal (that without any competition).

Table 3. Frequency of selected contact amino acid for 10 X-ray structures of anti-hapten antibodies[a]

Position	Region	Frequency (n/10)[b]
H33	FR2 H	5
H35		6
H50		5
H95	CDR H3	6
H96		7
H97		8
L50	CDR L2	2
L53		0
L89	CDR L3	2
L91		8
L92		1
L94		6
L96		8

[a] Study undertaken by MacCallum *et al.* (1996).
[b] Number of antibodies making contacts with hapten at each position.

9D3. Conversely, antibody 9D3 binds phenolic A-ring estradiol conjugates such as estradiol-3-sulphate and estradiol-3-glucuronide. Thus, antibody 9D3 is very specific for the D-ring but not for the A-ring of estradiol. Moreover, estradiol derivatives modified either at C6 (6-oxoestradiol or 6α/β-ANBA-estradiol photoreagents) or C7 (7-oxoestradiol, 7-CMO-estradiol) are recognized by the 9D3 antibody. Therefore, C6 and C7 positions are likely to be solvent exposed, as expected, at least for C7 position, through which the steroid hapten was linked to the immunogen. The high affinity ($K_a = 1.3 \times 10^{10}\ M^{-1}$ at 20 °C) of mAb 9D3 for estradiol measured by equilibrium dialysis suggests the existence of hydrogen bonds between the antibody 9D3 and estradiol. In summary, 9D3 has a strong affinity for estradiol and a high specificity for the D-ring but presents a lack of specificity for the C3 position which results in very high cross-reactivity with estradiol-3 conjugates.

Photoaffinity labelling experiments have been carried out on mAb 9D3 with different (5-azido-2-nitrobenzoyl)amido (ANBA) derivatives linked at C3, C6 and C7 positions of estradiol (Rolland de Ravel *et al.*, 2001) in order to explore the corresponding low specific regions of the paratope (Table 2). The 3-ANBA-EA-CMO-[17α-^{3}H]-estradiol (maximal photocross-linker length ~15 Å) photoreacted with the TyrL32 while the shorter 3-ANBA-ethyloxy-[17α-^{3}H]-estradiol (maximal photocross-linker length ~10 Å) was unreactive. These results suggest that a very large pocket exists around C3 and that the C3 position is exposed to solvent, in agreement with the high cross-reactivities observed with estradiol-3 conjugates. Both 6α- and 6β-ANBA-[17α-^{3}H]-estradiol epimers (maximal photocross-linker length ~8 Å) also photoreacted with TyrL32, suggesting that C6 is relatively close to CDR L1. Moreover, simultaneous photolabelling of TyrH50, only with the 6β-epimer, suggests that the side chain of this residue is probably more accessible from the β face of estradiol. The fact that the TyrL32 was also photoactivated with 7-ANBA-EA-CMO-[17α-^{3}H]-estradiol bearing the same 7-CMO linker than the immunogen (maximal photocross-linker length ~15 Å) indicates that the intermediate linker is close to CDR L1. These results show that TyrL32 residue is freely accessible from the C3, C6 and C7 positions of estradiol. These photoaffinity labelling studies combined with detailed analysis of the specificity profile have provided helpful experimental data for the docking of estradiol into the 9D3 paratope to build the Fv 9D3 model.

Site-directed mutagenesis of 9D3 scFv

The aim of the site-directed mutagenesis experiments was to

Table 2. Photoaffinity labelling experiments

Photoreagent	Photolabelled residue	Sequence localization
3-ANBA-EA-CMO-[17α-^{3}H]estradiol	TyrL32	CDR L1
3-ANBA-ethyloxy-[17α-^{3}H]estradiol	No labelling	
6β-ANBA-[17α-^{3}H]estradiol	TyrL32	CDR L1
	TyrH50	FR2 H
6α-ANBA-[17α-^{3}H]estradiol	TyrL32	CDR L1
7-ANBA-EA-CMO-[17α-^{3}H]estradiol	TyrL32	CDR L1

Table 4. Affinity and specificity of wild-type and scFv mutants

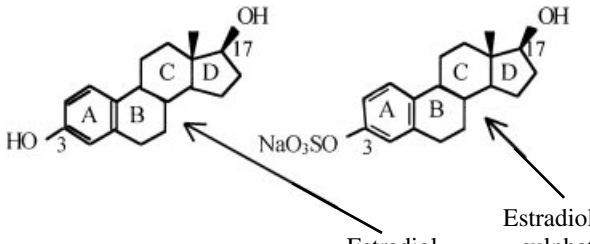

		Estradiol Affinity[a] (K_d nM)	Estradiol-3-sulphate Cross-reaction (%)[b]
Wild-type scFv		1.2	86
CDR H1	IleH33Met	2.0	200
	IleH33Leu	1.1	105
	GlnH35Lys	nb	nd
	GlnH35Asp	nb	nd
CDR H2	TyrH50Cys	1.3	72
	TyrH50Arg	0.8	280
CDR H3	ValH95Ala	6.6	180
	ValH95Leu	5.3	57
	AspH96Gln	nb	nd
	AspH96Glu	nb	nd
	GlyH97Ala	1.5	62
	GlyH97Val	50	nd
CDR L2	AsnL50His	0.5	95
	AsnL50Glu	0.5	62
	ThrL53Arg	1.1	85
	ThrL53Gly	0.9	80
	ThrL53Ser	1.8	76
CDR L3	HisL89Met	nb	nd
	HisL89Tyr	nb	nd
	TyrL91Cys	nb	nd
	TyrL91Phe	0.9	70
	SerL92Asp	0.5	82
	SerL92Ala	0.3	70
	IleL94Met	0.3	64
	IleL94Leu	6.0	100
	TrpL96Arg	nb	nd
Double-mutants			
GlyH97Ala/SerL92Asp		0.4	44
GlyH97Ala/IleL94Met		0.3	42
ValH95Leu/GlyH97Val		nb	nd

[a] Reported results are the mean of three independent experiments each made in triplicate. Affinities for estradiol were determined in solution by RIA and Scatchard analysis. The error, given for affinities for estradiol never exceeded 10%. nb: no binding.
[b] The percentage of cross-reaction was calculated as follows: (IC_{50} estradiol/ IC_{50} estradiol-3-sulphate) × 100. The IC_{50} is the concentration of steroid necessary to obtain 50% of the control signal (that without any competition). nd: not determined.

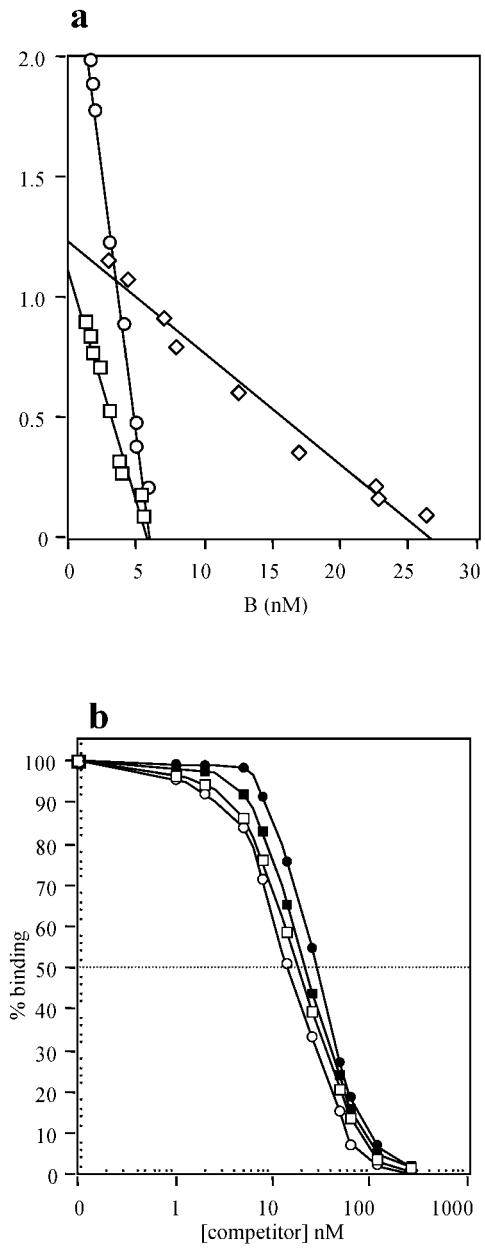

Figure 2. Determination of the affinities of wild-type scFv 9D3, GlyH97Val and GlyH97Ala/SerL92Asp scFv mutants. (a) scFv affinities were determined by radioimmunoassay and Scatchard analysis (□, wild-type; ◇, GlyH97Val; ○, GlyH97Ala/SerL92Asp). (b) The relative affinities of scFv were determined by radioimmunoassay in which binding to estradiol was inhibited by competitor: □, wild-type with estradiol competitor; ■, wild-type with estradiol-3-sulphate competitor; ○, GlyH97Ala/SerL92Asp with estradiol competitor; ●, GlyH97Ala/SerL92Asp with estradiol-3-sulphate competitor. The IC50 is the concentration of steroid necessary to obtain 50% of the control signal (that without any competition).

identify residues involved in the specific recognition of estradiol and to provide helpful atomic details toward building a molecular model. Mutations were performed on the high frequency contact residues (Table 3) determined from 10 X-ray structures of anti-hapten antibodies (MacCallum *et al.*, 1996), and on some other critical positions. In each case, the wild-type amino acid was replaced either by a bigger or a smaller amino acid as well as by an amino acid with a different polarity. The effects on binding affinity and specificity (Table 4) were measured using a tritiated unmodified estradiol structure chosen in order to obtain unambiguous data related exclusively to the interaction with the estradiol molecule. Binding affinity and cross-reactivity

Table 5. Activity of scFv, single domains and hybrid scFvs

V_H	V_L	Estradiol affinity[a] (K_d, nM)	Cross-reactions (%)[b]	
			Estradiol-3-sulphate	Estriol
9D3	9D3	1.2	86	0
15H11	15H11	0.5	0	90
	9D3	30	100	0
	15H11	nb	nd	nd
9D3		nb	nd	nd
15H11		nb	nd	nd
9D3	15H11	nb	nd	nd
15H11	9D3	1.5	238	0

[a,b] See table 4; nb: no binding; nd: not determined.

for the wild-type and mutant scFvs were estimated from binding curves, as illustrated in Fig. 2. The scFv mutants were classified according to the effect of the substitution on the affinity for estradiol and on the cross-reactivity with estradiol-3-sulfate.

The binding affinity of wild-type scFv 9D3 with estradiol (1.2 nM) was 10-fold lower than that measured for the monoclonal antibody and its cross-reactivity with estradiol-3-sulfate was significantly higher (86% instead of 51%). The GlnH35Lys, GlnH35Asp, AspH96Gln, AspH96Glu, HisL89Met, HisL89Tyr, TyrL91Cys and TrpL96Arg mutations were all found to abolish estradiol binding, thus revealing a first set of critical residues. The IleH33Leu, TyrH50Cys, TyrH50Arg, GlyH97Ala, ThrL53Arg, ThrL53Gly and TyrL91Phe mutations did not strongly affect binding affinity (in the range from 0.8 to 1.5 nM), but the cross-reactivity with estradiol-3-sulphate was the most significantly modified for the two mutants TyrH50Arg (strong increase to 280%) and GlyH97Ala (slight decrease to 62%). Mutants IleH33Met, ValH95Ala, ValH95Leu, GlyH97Val, ThrL53Ser and IleL94Leu exhibited decreased estradiol binding affinity, among which the two mutants ValH95Ala and ValH95Leu showed either an increased or a decreased cross-reactivity with estradiol-3-sulphate (180 and 57%, respectively). The AsnL50His, AsnL50Glu, SerL92Asp, SerL92Ala and IleL94Met mutations led to increased affinities for estradiol (in the range from 0.3 to 0.5 nM), among which the two AsnL50Glu and IleL94Met mutations were observed to slightly decrease the cross-reactivity with estradiol-3-sulphate (62 and 64%, respectively). Furthermore, the two double mutants GlyH97Ala/SerL92Asp and GlyH97Ala/IleL94Met, with one mutation on V_H and the other on V_L, were found to exhibit additive effects including an improved affinity for estradiol and a significantly decreased cross-reactivity (about 2-fold) with estradiol-3-sulfate (Table 4). However, the double mutant Val95Leu/GlyH97Val did not bind estradiol. In summary, mutant analysis suggests that a decreased cross-reactivity with estradiol-3-sulphate can be obtained by mutations on V_H while improved affinity can be obtained by mutations on V_L.

Leading role of V_L 9D3

To further assess the role of V_H and V_L domains, the two single V_H and V_L antibody fragments were constructed from mAb 9D3 and from mAb 15H11, a previously reported anti-estradiol antibody, with very different binding properties (Rousselot *et al.*, 1997). In addition, two chimeric scFvs corresponding to the V_H15H11/V_L9D3 and to the V_H9D3/V_L15H11 hybrids were also constructed. Binding properties of these antibody fragments, all produced in *E. coli*, were analysed by RIA with a tritiated estradiol tracer. The three V_H9D3, V_H15H11 and V_L15H11 single domains did not bind estradiol. Surprisingly, the single domain V_L9D3 was found to bind estradiol specifically, although with a low affinity (30 nM). Moreover, the cross-reactivity of the V_L9D3 domain for estradiol-3-sulphate was similar to the cross-reactivity of the scFv 9D3 (Table 5). These results suggest that V_L9D3 has a leading role for estradiol recognition. This hypothesis is supported by the observation that the hybrid V_H15H11/V_L9D3 scFv is active and binds estradiol with an affinity of 1.5 nM whereas the hybrid V_H9D3/V_L15H11 scFv is inactive. Moreover, the hybrid V_H15H11/V_L9D3 scFv cross-reacts with estradiol-3-sulphate (238%) but does not cross-react with estriol, a feature similar to the specificity profile observed for mAb 9D3, but opposite to the specificity of anti-estradiol antibody 15H11 which cross-reacts with estriol but not with estradiol-3-sulphate (Table 5). Other scFv hybrids were constructed with V_L9D3 in association with the V_H of the 5A4 anti-cortisol antibody (Le Calvez *et al.*, 1995) or of the V_H of the 1C11 anti-colicin antibody (Chames *et al.*, 1998b). These two latter scFv hybrids did not bind estradiol, thus indicating that association with improper VH domains can abolish estradiol recognition by VL9D3.

Comparative model of Fv 9D3 and docking of estradiol

Two possible alternative models (A and B) of Fv 9D3 were built using atomic coordinates of antibody fragments of D44.1 [Fig. 1(b); see Experimental Procedures]. The 9D3 sequence has a few peculiarities. First, in CDR L3, HisL89 is a scarcely observed residue (Pelleques JL, unpublished results), which is also present in another anti-estradiol 57-2 antibody (Lamminmäki *et al.*, 1997; Lamminmäki and Kankare, 2001). The HisL89 residue has been reported to stack above the conserved PheL98 ring making an amino–π interaction (Levitt and Perutz, 1988). Second, the presence

of TrpL96 imposes a particular conformation of CDR L3 in which the tryptophan side-chain points inward CDR L3. Third, CDR H3 is unusually short and contains only six amino acids with residues H99 and H100 missing (numbering according to Kabat or Chothia: www.bioinf.org.uk/abs/). Stereochemistry of the 9D3 models has been assessed using the PROCHECK program (Laskowski *et al.*, 1993). A Ramachandran plot is a good indicator of the quality of a model (Eu3D Validation Network, 1998). In 9D3, 86.4% of ϕ, ψ dihedral angles are located in the most favoured regions. The systematic outlier, AlaL51, is located in a disallowed region. The peptide bond planarity (7.5°) and the Cα chirality (1.5°) are within the typical values found in highly refined crystallographic structures. However, no refinement of the V_H–V_L interface was performed.

The docking of the estradiol molecule in the 9D3 binding site was done taking into account data from cross-reactivity measurements, photolabelling experiments, and site-directed mutagenesis studies. The much higher specificity of antibody 9D3 for the D-ring than for the A-ring or the C6 and C7 positions of estradiol is consistent with D-ring of estradiol deeply buried, whereas C3, C6 and C7 positions are solvent exposed. Estradiol could be docked along the narrow groove using two alternative orientations, one with the A-ring inserted either between CDR H3 and CDR L2 (model A), as found in the crystal structure of the rather similar anti-estradiol antibody 57-2 complexed with estradiol (Lamminmäki and Kankare, 2001), and the other one with A-ring between CDR L3 and CDR H2 (model B), as described in a previous molecular model of antibody 57-2 (Lamminmäki *et al.*, 1997; Plate 1). Both orientations are consistent with 9D3 cross-reactivity pattern, i.e. D-ring of estradiol deeply buried and C3, C6 and C7 position solvent exposed. In model A, estradiol α-face is stacked against the 9D3 V_L, whereas its β-face is stacked against the 9D3 V_H. According to the steroid orientation proposed in model A, the estradiol D-ring is located between CDR L3 and CDR H1. The 18-CH3 group is located in a shallow pocket created by ValH95 and GlyH97. In this model, the 17β-OH group of estradiol makes three hydrogen bonds ($d \leq 3.5$ Å) with TyrL36, HisL89, and GlnH35 [Plate 1(A)]. In model B, the estradiol molecule is rotated about 180°, compared with model A. Thus, the estradiol α-face is stacked against the 9D3 V_H whereas its β-face is stacked against the 9D3 V_L. In this orientation, the estradiol is docked along the narrow groove with the D-ring buried at the bottom of the binding site, close to CDR H3 [Plate 1(B)]. The 18-CH3 group is located in a shallow pocket created by the short side-chain of AlaL34. The estradiol is sandwiched by two side-chains, TyrL91 of CDR L3 stacking with β-face of estradiol and ValH95 of CDR H3, stacking with α-face. The 17β-OH group of estradiol can make a potential hydrogen bond with TyrL36 from FR2 L [Plate 1(B)].

DISCUSSION

Site-directed mutagenesis and docking of estradiol

In the two proposed comparative models of the Fv 9D3-estradiol complex, TyrL91, a central residue of the paratope offers a large contact surface either with the α-face of estradiol (model A) [Plate 1(A)] in a manner similar to that observed for PheL91 in the crystal structure of the Fab 57-2 estradiol complex (Lamminmäki and Kankare, 2001) or with the β-face of estradiol (model B) [Plate 1(B)] as also reported in the previous molecular model of antibody 57-2 (Lamminmäki *et al.*, 1997). Indeed, substitution of TyrL91Cys inactivates estradiol binding (Table 4), whereas substitution by phenylalanine (TyrL91Phe), another aromatic residue, did not change significantly the binding properties of 9D3. Opposite to TyrL91, the short CDR H3 interacts with the other face of estradiol through two non aromatic small residues: ValH95 and GlyH97. The two mutations ValH95Ala and ValH95Leu strongly decreased the binding affinity of 9D3 (Table 4). Interestingly, substitution of ValH95 by a smaller alanine residue strongly increased cross-reactivity with estradiol-3-sulphate as compared to the wild-type scFv (from 86 to 180%), whereas substitution by a bigger leucine residue decreased significantly the cross-reactivity with estradiol-3-sulphate (57%). In the two models A and B, ValH95, although much smaller than the homologous TrpH95 of 57-2 antibody, fills in a critical space between CDR H1, CDR H3 and estradiol. On the other hand, the slightly larger mutation GlyH97Ala led to a slight loss of affinity and also decreased significantly the cross-reactivity with estradiol-3-sulphate (62%) whereas the larger mutation GlyH97Val was found to induce the strongest loss of affinity observed in this study, presumably reflecting a steric effect preventing estradiol to penetrate into the paratope. Moreover, replacement of AspH96 by a Gln or by a Glu residue rendered mutants inactive (Table 4). This inactivation probably results from alteration of the conformation of CDR H3. Presumed contacts between 9D3 antibody site and estradiol, established from site-directed mutagenesis and molecular modelling, are listed in Table 6 for the two alternative orientations (models A and B) of estradiol. Ninety-four percent in model A (205 Å), and 90% in model B (197 Å) of the antigen surface is buried by the 9D3 antibody combining site despite the fact that atoms O3, C4, C6 and C7 of estradiol are partially solvent exposed in both models. The importance of V_L chain for conferring a high specificity for the D-ring might be explained either by the presence of two hydrogen bonds between 17β-OH of estradiol and the two TyrL36 and HisL-89 residues in model A [Plate 1(A)] or by the presence of a single hydrogen bond between 17β-OH and TyrL36 associated with a pocket created by the AlaL34, TyrL36, LeuL46, TyrL49 and TyrL91 which can accept the 17-OH and the 18-CH3 groups in model B [Plate 1(B)]. Among these five residues only TyrL91 was submitted to site-directed mutagenesis because other amino acids were not among those reported as the most frequent contact residues for anti-hapten antibodies (MacCallum *et al.*, 1996). It should be noted that studies on the catalytic 48G7 anti-hapten antibody, have demonstrated that AlaL34 is a key residue involved in the catalytic reaction through hapten binding (Wedemayer *et al.*, 1997). AsnL50 is a contact residue of the A-ring in model A, and of the D-ring in model B (Table 6). Interestingly, mutations AsnL50His and AsnL50Glu improved binding affinity of the antibody (0.5 nM) and decreased cross-reactivity with estradiol-3-sulfate (Table 4). In both models, the bottom of the binding pocket is formed by HisL89 and TrpL96 residues (Plate 1). These two residues are critical for

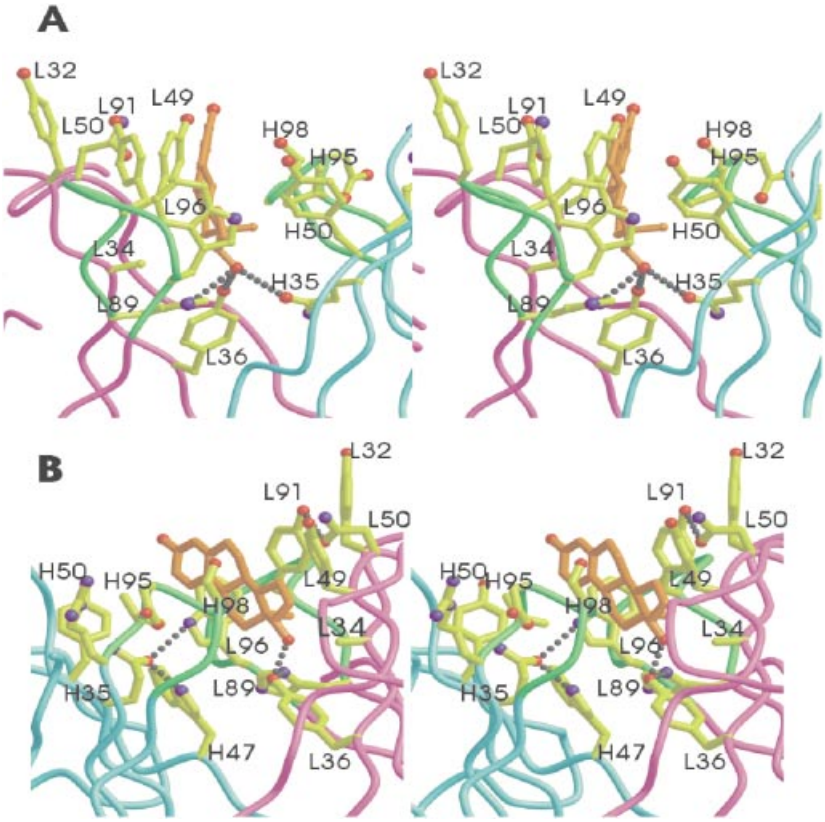

Plate 1. Stereo views of the two comparative models of 9D3 with docked estradiol (orange). Important side-chains are drawn in yellow ball-and-sticks. (A) In model A, the α-face of estradiol is stacked against the V_L 9D3 (magenta tube) and its β-face toward the V_H 9D3 (cyan tube). The estradiol A-ring, with its O3 atom, is partially solvent-exposed between CDR H3 (green tube) and CDR L2. Estradiol 17-OH makes three hydrogen bonds with TyrL36, HisL89, and GlnH35, represented by gray dots. (B) In model B, the β-face of the estradiol is stacked against the V_L 9D3 and its α-face toward the V_H 9D3. Estradiol 17-OH makes a single hydrogen bond with TyrL36 represented by gray dots. Hydrogen bonds between GlnH35, TrpH47, and TrpL96 are also drawn in gray. This figure is drawn using Molscript (Kraulis, 1991) and rendered by Raster3D (Merritt and Bacon, 1997).

Table 6. Contacts between estradiol and 9D3

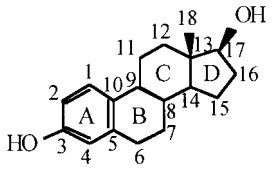

9D3		Estradiol (model A)			Estradiol (model B)		
Region	Residue	Face	Atom	Ring	Face	Atom	Ring
CDR H1	GlnH35	β	17-OH	D (H-bond)			
CDR H3	ValH95	β	C15,C16,C18	D	α	C1,C2,C9,C10,C11	A,B,C
	AspH96	β	C2,C3,C4	A			
	GlyH97	β	C1,C2,C9,C10,C11,C18	A,B,C,D	α	C14,C17	D
CDR L1	AlaL34				β	C16,C17,C18,17-OH	D
FR2 L	TyrL36	α	C12,17-OH	D (H-bond)	β	C17,17-OH	D (H-bond)
	TyrL49	α	C1,C2,C3,O3,C10	A	β	C15,C16	D
CDR L2	AsnL50	α	C1,C2,C3,O3,C10	A	β	C15	D
CDR L3	HisL89	α	C16,C17,17-OH	D (H-bond)	β	C12,C18	C
	TyrL91	α	C6,C7,C8,C9,C14,C15	B,C,D	β	C5,C6,C8,C11,C18	A,B,C,D
	TrpL96	α	C15,C16	D	β	C1,C2,C3	A

Presumed contacts between estradiol and the 9D3 antibody according to the docking of estradiol with the comparative models A and B of Fv 9D3.

estradiol recognition as shown by the loss of estradiol binding activity observed for mutants HisL89Met, HisL89Tyr, and TrpL96Arg (Table 4). In model A, HisL89 interacts with the 17β-OH group via hydrogen bonding whereas in model B it interacts with OH group of TyrL36 (Table 6 and Plate 1). In model A, TrpL96 interacts with the C15 and C16 atoms of estradiol [Plate 1(A)], whereas in model B it interacts with the C1 and C2 atoms of estradiol and makes a hydrogen bond with GlnH35. The two mutations SerL92Asp and IleL94Met in CDR L3 increased estradiol affinity of antibody 9D3 antibody from 1.2 nM to 0.5 and 0.3 nM, respectively (Table 4), in contrast to the mutation IleL94Leu which induced a strong loss of affinity. These residues are not in contact with estradiol in the two 9D3 models but were mutated because L94 is a high frequency contact residue (MacCallum *et al.*, 1996) and L92 is a contact residue of antibody DB3 antibody (Arevalo *et al.*, 1993). In the two models, the side-chain of SerL92 is located above the important contact residue TyrL91. Substitution of SerL92 by Asp may strengthen the stacking of TyrL91 on α-face of estradiol (model A) or on the β-face (model B) and thus improve the affinity. The IleL94 residue is located at the level of V_H–V_L interface and probably interacts with TyrH50, LysH59 and TrpH47 residues from the heavy chain. Therefore, a mutation such as IleL94Met, introduced at the V_H–V_L interface, known to play an important role in the antigen binding process (Pellequer *et al.*, 1999), may influence antibody binding affinity. GlnH35 also participates in model B to the V_H–V_L interactions by making a conserved hydrogen bond with TrpH47 and TrpL96 residues [Plate 1(B)] which are both known to be frequently in contact with hapten (MacCallum *et al.*, 1996). However, in model A, GlnH35 is a contact residue with estradiol which interacts by hydrogen bonding with the 17β-OH group of estradiol, as reported in the crystal structure from the Fab 57-2-estradiol complex. Site-directed mutagenesis showed that mutations GlnH35Lys and GlnH35Asp abolish the binding with estradiol, highlighting the critical structural role of GlnH35 (Table 4), particularly evident in model A. In model A, residues TyrL49 and AsnL50 in CDR L2 and SerH98 in CDR H3 are relatively close to the solvent exposed C3 position of estradiol [Plate 1(A)] and, therefore, could be expected to represent preferential targets in order to improve specificity for the 3-OH group by site-directed mutagenesis. Indeed, the mutation AsnL50Glu led to an increased affinity for estradiol and to a slightly decreased cross-reaction with estradiol-3-sulphate. In model B, the two residues TyrH50 in CDR H2 and IleH33 in CDR H1 which are relatively close to the solvent exposed C3 position of estradiol [Plate 1(B)] represent potential targets in order to improve specificity for the 3-OH group by site-directed mutagenesis. However, another possible way to remove cross-reactivity with estradiol-3-sulphate and 3-glucuronide conjugates could be random mutagenesis either of CDR L2 or of CDR H3 in the vicinity of C3 position in order to create an appropriate interaction with the 3-phenolic hydroxyl group of estradiol.

Leading role of the V_L

The 17β-OH group of estradiol is stabilized by three hydrogen bonds with TyrL36, HisL89 and GlnH35 in model A and by only one potential hydrogen bond with TyrL36, in model B, but in this latter case TyrL36 lies in a small hydrophobic pocket also formed with AlaL34 which accommodates both 17-OH and 18-CH3 groups. Therefore, based on these observations, both models are compatible

with the leading role of the V_L domain of 9D3 for estradiol recognition, demonstrated by the binding properties of the single V_L domain of 9D3 as well as of the V_H15H11/V_L9D3 hybrid which exhibited the same specificity profile as mAb 9D3, whereas the other single V_H9D3, V_H15H11 and V_L15H11 domains and the V_H9D3/V_L15H11 hybrid were totally inactive. The stabilizing role of the association of V_L9D3 with V_H15H11 on the binding properties of V_L9D3 might result from different factors such as the small length of CDR H3 (shorter in 15H11 than in 9D3) and the possibility that GlyH95 of 15H11 can be oriented towards the β- or α-face of estradiol like ValH95 for 9D3 in models A or B, respectively. Moreover, the association of V_L9D3 with V_H15H11 does not confer the specificity profile characteristic of antibody 15H11, but exclusively that of antibody 9D3, thus confirming that the V_L domain has a leading role for estradiol recognition. This predominant role of V_L was unexpected since the V_H domain is known to be most often involved in antigen recognition by anti-hapten antibodies. Generally, CDR H3 residues are responsible for the surface contact area and molecular interactions which contribute to antigen binding (Chothia and Lesk, 1987; Chothia *et al.*, 1989; Padlan, 1994). The capacity of the V_L domain to retain the binding properties is rarely observed. To our knowledge, only one example seems to have been previously reported for the V_L domain of anti-dsDNA autoantibodies (Suzuki *et al.*, 2000), while another related but less representative example concerns the V_L domain of the anti-vasoactive intestinal polypeptide catalytic antibody Fv, on which are located the essential catalytic residues (Sun *et al.*, 1997). In antibody 57-2, the V_L domain, which has 90% identity with that of 9D3, also plays an important role in the recognition of estradiol (Lamminmäki and Kankare, 2001).

Comparison of the scFv 9D3-estradiol complex with other antibody-steroid complexes

The structural data firmly established from X-ray structures of the three DB3 anti-progesterone (Arevalo *et al.*, 1993), 26-10 anti-digoxin (Jeffrey *et al.*, 1993), and 4155 anti-estrone-3-glucuronide (Trinh *et al.*, 1997) antibodies highlight several common characteristics. First, aromatic residues always stack with the steroid skeleton. Second, V_H plays a prominent role in hapten recognition by these three anti-steroid antibodies. For instance, V_H of 26-10 anti-digoxin Fab contributes to 75% of total buried area, V_H of 4155 Fv, directed against estrone-3-glucuronide, accounts for 81% of the total buried area, with more than 40% due to the CDR H3, and finally, the B-, C- and D-rings of progesterone are deeply embedded in a hydrophobic cavity created by TrpH47, TrpH50, TyrH97, TrpH100 and PheH100b making 60% of the total buried area in the DB3 antibody. The recognition of estradiol by 9D3 antibody is unusual because in this case it is the V_L region, which interacts predominantly with the antigen, while, in both models, only ValH95 and GlyH97 belonging to the CDR H3 are contact residues. In particular, CDR L2 of 9D3 is important for estradiol recognition, unlike in DB3, 4155 and 26-10 antibodies. The opposite orientations of estradiol in the two comparative models of antibody 9D3 correspond to that firmly established from the crystal structure of the Fab 57-2-estradiol complex (Lamminmäki and Kankare, 2001), for model A, and to that previously proposed in a previous comparative model of the anti-estradiol 57-2 antibody (Lamminmäki *et al.*, 1997), for model B, as expected from rather similar overall binding specificity profiles, even though 9D3 antibody, generated with an estradiol-7-CMO-BSA immunogen, has a higher affinity for estradiol ($1.3 \times 10^{10}\ M^{-1}$) than 57-2 antibody, generated with estradiol-6-CMO-BSA ($3.9 \times 10^{8}\ M^{-1}$). Both antibodies are highly specific for the D-ring of estradiol and present also a similar lack of specificity for the C3 position. Antibody 9D3 cross-reacts with estradiol-3-sulphate (51%) and estradiol-3-glucuronide (28%) but not with testosterone, while antibody 57-2 cross-reacts less than 9D3 with estradiol-3-sulphate (7%) and estradiol-3-glucuronide (23%), but shows a rather high cross-reactivity with testosterone (37%). Antibody 9D3 cross-reacts strongly with both C6 and C7 substituted derivatives of estradiol whereas antibody 57-2 cross-reacts only with C6 analogues, but much more than with estradiol, in the latter case. These observations as well as other cross-reactivity measurements indicate that, for both antibodies 9D3 and 57-2, the C3, C4, C5, C6 and C7 of estradiol are all exposed to the solvent whereas the D-ring is inserted at the bottom of the combining site. Sequence alignments reveal a very high sequence identity of V_L domains (90% restricted to 75 for the CDR L3), including the presence in both antibodies of the atypic HisL89 residue. A much lower homology was observed for the V_H domains (51%). The binding properties of the single V_L9D3 domain and of the V_L9D3/ V_h15H11 hybrid scFv indicate that the specificity of 9D3 antibody for the D-ring is conferred mostly by the V_L, whereas the crystal structure of antibody 57-2 shows that the specificity for the D-ring is conferred partially by V_L but also involves V_H (proposed hydrogen bond of 17-OH group with GlnH35). Therefore, even though antibodies 9D3 and 57-2 have several common features, further studies are obviously needed to provide direct evidence supporting the choice either of model A, in which the estradiol orientation is similar to that observed in the crystal structure of the Fab 57-2-estradiol complex, or of model B, in which estradiol is rotated about 180°, compared with model A. It should be noted that the two possible orientations remain consistent with data from cross-reactivity measurements, photoaffinity labelling and mutagenesis studies, even though photoaffinity labelling results with 6α/β-derivatives are slightly more in favour of model A. Nevertheless, taken together, these results provide potentially important information for the design of appropriate strategies for reshaping the combining site of anti-estradiol antibodies by antibody engineering methodologies.

CONCLUSIONS

We developed an integrated approach to the rational design of antibodies with improved affinities and specificities by combining radio-ligand binding assays, photoaffinity labelling, site-directed mutagenesis, comparative modelling, and ligand docking. We have shown that the reactivity of 9D3 with estradiol depends essentially on: (i) the interactions

between α- and β-faces of estradiol with TyrL91 and ValH95, respectively, for model A or with ValH95 and TyrL91 for model B; (ii) the presence of hydrogen bonds stabilizing the 17β-OH group of estradiol, either with TyrL36, HisL89, and GlnH35 if estradiol is oriented as in model A or of a deep pocket created by the AlaL34, TyrL36, LeuL46, TyrL49, and TyrL91 encompassing a possible hydrogen bond between TyrL36 and 17-OH if estradiol is oriented as in model B; (iii) the structural role of HisL89 and TrpL96 residues; (iv) the fact that the phenolic 3-OH group of estradiol remains solvent exposed, explaining the lack of specificity against the 3-substituted-estradiol derivatives. Some key residues, which could be involved in cross-reactivity with estradiol-3-sulphate, emerge from the 9D3 models. This knowledge could be helpful to elaborate a strategy to design mutants devoid of cross-reactivity with estradiol-3-sulphate and estradiol-3-glucuronide conjugates. Random mutagenesis of the CDR H3 close to the C3 position and of CDR L2 might allow estradiol skeleton to penetrate more deeply in the paratope in order to create new interactions with the 3-OH group to decrease cross-reactivity with estradiol-3 derivatives. A parallel strategy has been reported in the case of antibody 57-2, based on elongation of the CDR H2 loop which was successful to annihilate the cross-reactivity with testosterone (Lamminmäki *et al.*, 1999).

Acknowledgements

We thank Jean-Yves Métais for critical reading and discussions. This work was supported by the French National Center for Scientific Research (CNRS, grant ACCSV5- 9505207).

REFERENCES

Arevalo JH, Stura EA, Taussig MJ, Wilson IA. 1993. Three-dimensional structure of an anti-steroid Fab' and progesterone-Fab' complex. *J. Mol. Biol.* **231**: 103–118.

Arevalo JH, Hassig CA, Stura EA, Sims MJ, Taussig MJ, Wilson IA. 1994. Structural analysis of antibody specificity. Detailed comparison of five Fab'-steroid complexes. *J. Mol. Biol.* **241**: 663–690.

Bhat TN, Bentley GA, Fischmann TO, Boulot G, Poljak RJ. 1990. Small rearrangements in structures of Fv and Fab fragments of antibody D1.3 on antigen binding. *Nature* **347**: 483–485.

Braden BC, Souchon H, Eisele JL, Bentley GA, Bhat TN, Navaza J, Poljak RJ. 1994. Three-dimensional structures of the free and the antigen-complexed Fab from monoclonal anti-lysozyme antibody D44.1. *J. Mol. Biol.* **243**: 767–781.

Brooks B, Bruccoleri R, Olafson B, States D, Swaminathan S, Karplus M. 1983. CHARMM: A program for macromolecular energy, minimization, and molecular dynamics calculations. *J. Comp. Chem.* **4**: 187–217.

Brünger AT. 1992. *X-PLOR Manual. Version 3.0.* Yale University Press: New Haven, CT.

Chames P, Coulon S, Baty D. 1998a. Improving the affinity and the fine specificity of an anti-cortisol antibody by parsimonious mutagenesis and phage display. *J. Immunol.* **161**: 5421–5429.

Chames P, Fieschi J, Baty D, Duche D. 1998b. Intracellular immunization of prokaryotic cells against a bacteriotoxin. *J. Bacteriol.* **180**: 514–518.

Chen Y, Wiesmann C, Fuh G, Li B, Christinger HW, McKay P, de Vos AM, Lowman HB. 1999. Selection and analysis of an optimized anti-VEGF antibody: crystal structure of an affinity-matured Fab in complex with antigen. *J. Mol. Biol.* **293**: 865–881.

Chothia C, Lesk AM. 1987. Canonical structures for the hypervariable regions of immunoglobulins. *J. Mol. Biol.* **196**: 901–917.

Chothia C, Lesk AM, Tramontano A, Levitt M, Smith-Gill SJ, Air G, Sheriff S, Padlan EA, Davies D, Tulip WR *et al.* 1989. Conformations of immunoglobulin hypervariable regions. [See comments.] *Nature* **342**: 877–883.

Eu 3-D Validation Network. 1998. Who checks the checkers? Four validation tools applied to eight atomic resolution structures. *J. Mol. Biol.* **276**: 417–436.

Gani M, Coley J, Piron J, Humphreys AS, Arevalo J, Wilson IA, Taussig MJ. 1994. Monoclonal antibodies against progesterone: effect of steroid-carrier coupling position on antibody specificity. *J. Steroid Biochem. Mol. Biol.* **48**: 277–282.

Geisler J, Berntsen H, Lonning PE. 2000. A novel HPLC-RIA method for the simultaneous detection of estrone, estradiol and estrone sulphate levels in breast cancer tissue. *J. Steroid Biochem. Mol. Biol.* **72**: 259–264.

Hoogenboom HR, Griffiths AD, Johnson KS, Chiswell DJ, Hudson P, Winter G. 1991. Multi-subunit proteins on the surface of filamentous phage: methodologies for displaying antibody (Fab) heavy and light chains. *Nucl. Acids Res.* **19**: 4133–4137.

Horton RM, Hunt HD, Ho SN, Pullen JK, Pease LR. 1989. Engineering hybrid genes without the use of restriction enzymes: gene splicing by overlap extension. *Gene* **77**: 61–68.

Jeffrey PD, Strong RK, Sieker LC, Chang CY, Campbell RL, Petsko GA, Haber E, Margolies MN, Sheriff S. 1993. 26-10 Fab-digoxin complex: affinity and specificity due to surface complementarity. *Proc. Natl Acad. Sci. USA* **90**: 10310–10314.

Kabat EA, Wu TT, Perry HM, Gottesman KS, Foeller C. 1991. *Sequences of Proteins of Immunological Interest*, 5th edn. NIH: Bethesda, MD.

Kraulis PJ. 1991. MOLSCRIPT: a program to produce both detailed and schematic plots of protein structures. *J. Appl. Crystallogr.* **24**: 946–950.

Lamminmäki U, Villoutreix BO, Jauria P, Saviranta P, Vihinen M, Nilsson L, Teleman O, Lövgren T. 1997. Structural analysis of an anti-estradiol antibody. *Mol. Immunol.* **34**: 1215–1226.

Lamminmäki U, Pauperio S, Westerlund-Karlsson A, Karvinen J, Virtanen PL, Lövgren T, Saviranta P. 1999. Expanding the conformational diversity by random insertions to CDRH2 results in improved anti-estradiol antibodies. *J. Mol. Biol.* **291**: 589–602.

Lamminmäki U, Kankare JA. 2001. Crystal structure of a recombinant anti-estradiol Fab fragment in complex with 17 β-estradiol. *J. Biol. Chem.* **276**: 36687–36694.

Laskowski RA, MacArthur MW, Moss DS, Thornton JM. 1993. PROCHECK: A program to check the stereochemical quality of protein structures. *J. Appl. Crystallogr.* **26**: 283–291.

Le Calvez H, Fieschi J, Green JM, Marchesi N, Chauveau J, Baty D. 1995. Paratope characterization by structural modelling of two anti-cortisol single-chain variable fragments produced in *E. coli*. *Mol. Immunol.* **32**: 185–198.

Levitt M, Perutz MF. 1988. Aromatic rings act as hydrogen bond acceptors. *J. Mol. Biol.* **201**: 751–754.

MacCallum RM, Martin AC, Thornton JM. 1996. Antibody-antigen interactions: contact analysis and binding site topography. *J. Mol. Biol.* **262**: 732–745.

Marks JD, Griffiths AD, Malmqvist M, Clackson TP, Bye JM, Winter G. 1992. By-passing immunization: building high affinity human antibodies by chain shuffling. *Biotechnology* **10**: 779–783.

McRee DE. 1992. XtalView: A visual protein crystallographic software system for XII/Xview. *J. Mol. Graph.* **10**: 44–47.

Merritt EA, Bacon DJ. 1997. Raster3D: Photorealistic molecular

graphics. *Meth. Enzymol.* **277**: 505–524.
Miller JH. 1992. *A Short Course in Bacterial Genetics, a Laboratory Manual and Handbook for Escherichia coli and Related Bacteria*. Cold Spring Harbor Laboratory Press: Cold Spring Harbor, NY; 439.
Padlan EA. 1994. Anatomy of the antibody molecule. *Mol. Immunol.* **31**: 169–217.
Pellequer JL, Chen SWW, Roberts VA, Tainer JA, Getzoff ED. 1999. Unraveling the effect of changes in conformation and compactness at the antibody V_L–V_H interface upon antigen binding. *J. Mol. Recogn.* **12**: 267–275.
Plückthun A. 1991. Antibody engineering: advances from the use of *Escherichia coli* expression systems. *Biotechnology* **9**: 545–551.
Roberts VA, Stewart J, Benkovic SJ, Getzoff ED. 1994. Catalytic antibody model and mutagenesis implicate arginine in transition-state stabilization. *J. Mol. Biol.* **235**: 1098–1116.
Rolland de Ravel M, Blachère T, Delolme F, Dessalces G, Coulon S, Baty D, Grenot C, Mappus E, Cuilleron CY. 2001. Specific photoaffinity labelling of Tyr-50 on the heavy chain and of Tyr-32 on the light chain in the steroid combining site of a mouse monoclonal anti-estradiol antibody using C3-, C6-, and C7-linked 5-azido-2-nitrobenzoylamidoestradiol photoreagents. *Biochemistry* **40**: 14907–14920.
Roussel A, Cambillau C. 1989. Turbo-Frodo. In *Silicon Graphics Geometry Partners Directory*. Silicon Graphics: Mountain View, CA.
Rousselot P, Mappus E, Blachère T, Rolland de Ravel MR, Grenot C, Tonnelle C, Cuilleron CY. 1997. Specific photoaffinity labelling of Tyr-49 on the light chain in the steroid-combining site of a mouse monoclonal anti-estradiol antibody using two epimeric 6alpha- and 6beta-(5-azido-2-nitrobenzoyl)amidoestradiol photoreagents. *Biochemistry* **36**: 7860–7868.
Skerra A, Plückthun A. 1988. Assembly of a functional immunoglobulin Fv fragment in *Escherichia coli*. *Science* **240**: 1038–1041.
Sun M, Gao QS, Kirnarskiy L, Rees A, Paul S. 1997. Cleavage specificity of a proteolytic antibody light chain and effects of the heavy chain variable domain. *J. Mol. Biol.* **271**: 374–385.
Suzuki M, Takemura H, Suzuki H, Sumida T. 2000. Light chain determines the binding property of human anti-dsDNA IgG autoantibodies. *Biochem. Biophys. Res. Commun.* **271**: 240–243.
Trinh CH, Hemmington SD, Verhoeyen ME, Phillips SE. 1997. Antibody fragment Fv4155 bound to two closely related steroid hormones: the structural basis of fine specificity. *Structure* **5**: 937–948.
Tuffery P, Etchebest C, Hazout S, Lavery R. 1991. A new approach to the rapid determination of protein side chain conformations. *J. Biomol. Struct. Dyn.* **8**: 1267–1289.
Wedemayer GJ, Wang LH, Patten PA, Schultz PG, Stevens RC. 1997. Crystal structures of the free and liganded form of an esterolytic catalytic antibody. *J. Mol. Biol.* **268**: 390–400.
Whitlow M, Bell BA, Feng SL, Filpula D, Hardman KD, Hubert SL, Rollence ML, Wood JF, Schott ME, Milenic DE *et al.*, 1993. An improved linker for single-chain Fv with reduced aggregation and enhanced proteolytic stability. *Protein Engng* **6**: 989–995.
Yoon DY, Choi MJ, Choe IS, Chung TW, Byun SM. 1993. Influence of the conjugation site on the specificity of monoclonal antibodies to progesterone and on the performance of direct enzyme immunoassay. *Biochem. Mol. Biol. Int.* **31**: 553–563.

